CHAPTER 3

FOREST CHANGE DETECTION BY WINTER SATELLITE IMAGES

3.1 Background

In the Russian Far East, forest resources have been consistently diminishing since the Soviet era through exploitation or other disturbance (Section 2.1). Thus, there is a need for remote sensing to provide an independent means of detecting and evaluating disturbances in boreal forests. Forest cuts and other canopy removal can be detected on satellite images by change detection (Section 1.3). In the Russian Far East, satellite images have been acquired frequently only in winter (Sections 1.4, 2.1). However, Snow-covered satellite images can be used for the monitoring and inventory of boreal forests as a stable data source (Section 2.2). In response to the consideration above, this Chapter aims the followings;

- To find appropriate image indices for canopy change detection in boreal forest using winter satellite images with snow.
- To distinguish the winter indices from the summer indices in terms of forest change detection and recovery detection.

3.2 Study Area

The study area is at the western skirt of the Sikhote-Alin Range, east of Khabarovsk, in the Russian Far East (Figure 3.1). The area covers a square of ca 180 km by 180 km within a Landsat scene (path/row = 121/026 in WRS-2). Lowland of marsh and grassland along the Amur River predominates in the western part of the area, while forest covers the slopes of the range in the eastern part. The altitude ranges from about 30 m near the Amur River to more than 2000 m in the range. The Japan Forest Technology Association (JAFTA, 1998) carried out a forest resource study using satellite images in the same area.

In Khabarovsk, the monthly mean temperature is below 0 ℃ from November through March, and the minimum temperature is –20.9 ℃ in January (National Astronomical Observatory, 1997). Precipitation from April to September accounts for

more than 80% of the annual amount of 678.8 mm, which makes the probability of acquiring cloud-free satellite images here much greater in winter than in summer (TAKAO, 2000). At the Gassinski Model Forest, which is within the study area, the snow depth reaches 40 to 50 cm and winter snow cover lasts 150 days (Gassinski Model Forest Association, WWW).

The forest consists of coniferous and deciduous broadleaf species. The main species distributed in the area are Dahurian larch (*Larix gmelinii*), Ezo spruce (*Picea jezoensis*), fir (*Abies nephrolepis*), Korean pine (*Pinus koraiensis*) ash (*Fraxinus mandshurica*), linden (*Tilia amurensis*), oak (*Quercus mongolica*), elm (*Ulmus davidiana*) and birch (*Betula costata*) (OKITSU, 1997).

Some scenery of the forests and trees are depicted in Photo 3.1 – 3.6.

3.3 Methods

3.3.1 Images Used

The satellite images used in this study were five Landsat winter images (one MSS and four TM) along with one summer Landsat TM image. All were taken between 1980 and 1999 (Table 3.1, Figure 3.2). All the winter images were taken in mid-March, except for the 1999 image, which was taken in mid-February. The summer image was used for comparison of indices between winter and summer, as will be described.

Hereinafter, each ID in Table 3.1 will refer to the corresponding image. Note that TM95S is the one summer image.

3.3.2 Image Pre-Processing

TM96 was geocoded using ground control points (GCPs) collected on 1:200,000 topographic maps. All other images were related to TM96 using GCPs collected on screen, and then they were overlaid onto TM96 either by nearest-neighbor interpolation for the TM images or by cubic convolution for MSS80. The RMS error of GCPs for each overlay was less than one pixel.

Appropriate radiometric corrections were applied separately as described later. When reflectance for each wavelength is required in order to obtain an index, the

exoatmospheric reflectance is derived from pixel values with either the original (MARKHAM and BARKER, 1986) or the latest (MARKHAM and CHANDER, 2003) conversion parameters.

3.3.3 Index Selection

In this study, the single bands of the sensors and some commonly used indices were examined. Since MSS lacks mid-infrared bands, some indices could not be derived for MSS80.

1) Single bands (*RED*, *NIR*, *MIR*): A visible (MSS band 5, TM band 3), a near-infrared (MSS band 7, TM band 4), and a mid-infrared (TM band 5) were used. For all bands, the dark matter retrieval (CHAVEZ and MACKINNON, 1994) was applied as the atmospheric correction, and then converted into surface reflectance. Hereinafter, those three reflectances are referred to as *RED*, *NIR*, and *MIR*, respectively.
2) Normalized red band (*N-RED*): Prior to change detection by differencing of two successive images, these images needed to be mutually normalized such that the differences of 'no-change' points would distribute around zero. Empirical normalization using "pseudoinvariant features" is often used (SCHOTT *et al.*, 1988; HALL *et al.*, 1991; HEO *et al.*, 2000; DU *et al.*, 2002). At visible wavelengths, the reflectance of snow is very high and stable (DOZIER, 1989). Using the brightest snow and darkest matter, the visible band was normalized to a relative reflectance between 0 and 1. Because pixel values of MSS80's band 5 saturated at lower reflectance than most of the snow on the image, the pixel values corresponding to the brightest snow could not be derived. Instead, *N-RED* for MSS80 was derived by the inverse fitting of the regression from MSS80's band 5 to *N-RED* for TM85.
3) Normalized difference vegetation index (*NDVI*): *NDVI* was derived by equation (3.1) using *RED* and *NIR*;

$$NDVI = \frac{NIR - RED}{NIR + RED} \tag{3.1}$$

4) Normalized difference snow index (*NDSI*): *NDSI* is the analog of *NDVI*, which detects the snow cover by using the visible and mid-infrared bands. It was derived by equation (3.2) (KLEIN *et al.*, 1998).

$$NDSI = \frac{MIR - GRN}{MIR + GRN} \tag{3.2}$$

where *GRN* is the reflectance of TM band 2.

5) The robust vegetation and snow indices of SAITO and YAMAZAKI (1999): Combining *RED*, *NIR* and *MIR*, they proposed a vegetation index that is insensitive to the floor condition, *V2*, and a snow index that is insensitive to the overstory, *S3*. They noted that both indices could express the density of vegetation above snow cover.

$$V2 = \frac{NIR - RED}{NIR + MIR + RED} \tag{3.3}$$

$$S3 = \frac{NIR(RED - MIR)}{(NIR + RED)(NIR + MIR)} \tag{3.4}$$

6) Tasseled Cap (KAUTH and THOMAS, 1976; CRIST *et al.*, 1985): Tasseled Cap is a set of linear transformations of Landsat images that creates a new set of images from a TM image: *Brightness*, *Greenness*, *Wetness* and other components. Since the combination of these three components describes the degree of forest regeneration stage while reducing atmospheric influences, they have been widely used for forest change detection and monitoring (COHEN *et al.*, 1995; COLLINS and WOODCOCK, 1996; COHEN *et al.*, 1998). In this study, those three indices were derived from the original DN of the TM images without any atmospheric corrections.

3.3.4 Reference Data and Sampling

There was no independent vegetation information of the study area at hand,

nor did the author spend enough time in the area for data collection. However, in forest change detection, visual change interpretation of the image is a reliable means of developing reference data (COHEN *et al.*, 1998; HAYES and SADAR, 2001; WILSON and SADER, 2002).

The RGB composite technique (SADER and WINNE, 1992) with the time series of visible bands was used to delineate the forest canopy change. In this study, two color composites of the red bands (*1980 – 1985 – 1990* and *1990 – 1996 – 1999* for Blue – Green – Red, respectively) were provided for the interpretation. Since a forest stand becomes brighter in the red band after canopy removal, cuts or fires appear yellowish (at the first time period) or reddish (at the second time period) on the composites. By this interpretation, one of four disturbed periods (*1980 – 1985, 1985 – 1990, 1990 – 1996, 1996 – 1999*) was assigned to each canopy removal.

It was quite difficult to distinguish between cuts and fires using only band/index values, or pixel color, because in winter images the snow obscures the ground on which charcoal and ash are left after fire (ROY *et al.*, 2002). By interpretation, however, cuts and fire scars appear as quite different shapes (JAFTA, 1998): Cuts appear small with complex edges, whereas fire scars appear relatively large with round edges along topography. For comparison between cut and fire, fire scars were classified separately from cut stands.

The whole image was divided into 9-km by 9-km (300-px by 300-px) grids as the units of interpretation. First, the grids that the author visited or observed from air were interpreted. Then grids were randomly chosen for interpretation one by one until at least 120 sample points (described next) could be randomly collected for each disturbed period.

In each disturbed period, each sample point was randomly chosen from the center of a continuous area of the disturbed period where at least 5 by 5 neighboring pixels were assigned to the same disturbed period, and the sample value was derived as the average of the 3 by 3 neighboring pixels. While this approach may lead to a bias to overselection of larger cuts/fires, it avoids the errors of image overlay. The value was obtained at 60 points for each disturbed period, for index distribution estimation.

Another set of 60 points for each disturbed period was reserved for the producer's accuracy assessment of the classification (described in Subsection 3.5.3).

3.3.5 Separability and Stability of the Indices

The primary concern was whether the cut or burned stands were clearly separated from intact forest on the indices of each image. Though 'intact forest' could not be interpreted, the forest stands before cut were assumed to be intact. The separability of indices among forests, cuts and fires was evaluated.

The separability was measured as the probability of error in classification, assuming that the sample values of the indices were normally distributed (SWAIN, 1978). Suppose that there are two different normal distributions, represented by two normal probability density functions, $N_{\mu_1,\sigma_1}(x)$ and $N_{\mu_2,\sigma_2}(x)$ where the means or standard deviations are different from each other, i.e. $\mu_1 \neq \mu_2$ or $\sigma_1 \neq \sigma_2$, then the probability of error between the two distributions, P_e, is calculated by equation (3.5) or (3.6). P_e takes a value between 0 and 0.5, where the lower is P_e the better is the separability (Figure 3.4 (a)).

(if $\sigma_1 = \sigma_2$, assuming $\mu_1 < \mu_2$)

$$P_e = \int_{-\infty}^{\frac{\mu_1+\mu_2}{2}} N_{\mu_2,\sigma_2}(x)dx \tag{3.5}$$

(if $\sigma_1 \neq \sigma_2$)

$$P_e = \frac{1}{2}\left(\int_{-\infty}^{x_1} N_{\mu_1,\sigma_1}(x)dx + \int_{x_1}^{x_2} N_{\mu_2,\sigma_2}(x)dx + \int_{x_2}^{\infty} N_{\mu_1,\sigma_1}(x)dx \right) \tag{3.6}$$

where $x_1 < x_2$ are the solutions to the following equation

$$\left(\frac{1}{\sigma_1^2} - \frac{1}{\sigma_2^2}\right)x^2 - 2\left(\frac{\mu_1}{\sigma_1^2} - \frac{\mu_2}{\sigma_2^2}\right)x + \frac{\mu_1^2}{\sigma_1^2} - \frac{\mu_2^2}{\sigma_2^2} + \ln\frac{\sigma_1^2}{\sigma_2^2} = 0$$

Intact forests and snowfields are stable objects in terms of landuse throughout the satellite observations. In contrast, cut stands and fire scars can be less stable due

to the early succession of vegetation after the disturbances. If indices from the stable objects remain stable throughout the observations, a change in indices could suggest a real change in landuse. As an indicator of stability, the relative ranges of means for the land use classes were calculated. The relative range of means, RR_k for class $k \in$ {'forest,' 'cut/fire,' 'snow'} was calculated from a set of index means $\hat{I}_{i,j}$ for image i and class j as,

$$RR_k = \frac{\max\left(\hat{I}_{i,k}\right) - \min\left(\hat{I}_{i,k}\right)}{\max\left(\hat{I}_{i,j}\right) - \min\left(\hat{I}_{i,j}\right)} \qquad (3.7)$$

$$i = 1,2,\cdots, j = \text{'forest', 'cut/fire', 'snow'}$$

The more stable is an index is for its class, the lower is the RR_k (Figure 3.4 (b)).

3.3.6 Trend of Recovery through Chronosequence of Cut/Fire on an Image

Unlike following changes in certain samples through a time series of images, chronosequences of cuts were used to observe changes by comparing the index values of cut stands at different ages after cut on an image. To allow comparison among different samples, the method assumes that all samples of different age have identical conditions except the age. Actually, the conditions of atmosphere, snow, or sun location are more homogeneous within a single image than at a specific location among images of different dates.

Separability was calculated between intact forest and other classes. In addition, linear regression was applied from the mean age after cut to the index value, to find the trends of the index change after cut. When the regression is not significant, it suggests that the index is stable over time, or the change in the index is not linear. When the regression is significant, the age of recovery is calculated. The age of recovery is the age after cut on the regression line at which the index value becomes equal to the mean index value of intact forest.

Note that the 'recovery' discussed here is purely on the index basis. From the

viewpoint of forest succession, in general, 'soft' broadleaf species, such as birches and alders, are the first to regenerate, predominating for the first couple of decades after forest disturbance, after which they are gradually replaced by 'hard' broadleaf species and conifers over the course of centuries (KAKIZAWA, 2002a). One must remember that a boreal forest does not recover to nearly 'intact' within a few decades after severe disturbance.

A winter image, TM96, was used for the chronosequential analysis. A summer TM image, TM95S, was taken nine month earlier than TM96. A set of indices from TM95S identical to those from TM96 was derived for comparison with the results of the TM96. The time series of summer TM images could not be provided because of their lack of availability (TAKAO, 2000).

3.4 Results

3.4.1 The Interpreted Classes

Cuts were interpreted from each period of the time-series images. Large-scale fires occurred only between 1980 and 1985. Although relatively small areas of fire scar appeared on the fringes of large scars, they seemed to be dead trees that had fallen long after dying in the initial fires. In addition to these disturbances, open snowfields through all periods were arbitrarily interpreted. Finally, six classes were assigned for interpretation: *Cut 1980 – 1985*, *Cut 1985 – 1990*, *Cut 1990 – 1996*, *Cut 1996 – 1999*, *Fire 1980 – 1985*, and *Snow*.

These classes were divisible into *Before cut* and *After cut/fire* for each image at image acquisition, because the time of cut/fire was known. For the chronosequential analyses on TM96 and TM95S, these six classes above could be converted into *11 – 16 years after cut*, *6 – 11 years after cut*, *0 – 6 years after cut*, *Before cut*, *11 – 16 years after fire*, and *Snow*, respectively.

3.4.2 Separability of Cut/Fire from Intact Forest and the Stability of the Indices

The changes of the indices over time are shown in Figure 3.6. On TM85, TM90, and TM96, which had both *Before cut* and *After cut/fire* classes, the separability

between these classes was derived (Table 3.2). *RED*, *NIR*, *N-RED*, and the Tasseled Cap indices showed good separability, whereas *MIR* did not. The probabilities of error of *NDVI*, *V2*, *NDSI*, and *S3* varied widely among the images. These index values of intact forest were especially unstable.

Relative ranges showed that *NDVI*, *V2*, *NDSI*, and *S3* of the forests were very unstable. Relative ranges of *N-RED* and Tasseled Cap indices were relatively low for all the classes.

Cut 1980 – 1985 and *Fire 1980 – 1985* were poorly separated by any index, throughout the images. The probabilities of error ranged from 37% to 43% for TM85 immediately after disturbance, and decreased slightly with time to between 23% and 35% for TM99.

3.4.3 Trend of Recovery through Chronosequence of Cut/Fire on an Image

The chronosequences of the indices on TM96 and TM95S are shown in Figure 3.7. Table 3.3 shows the separability between intact forests (*Before cut*) and disturbances and the trend of the indices after cut. The summer *N-RED* was not derived for TM95S, since there were no stable bright and dark 'pseudoinvariant' objects on the ground in the summer image. The values of the winter *N-RED* should be identical to those of the winter *RED* in Table 3.3, based on the definition of both.

For the winter image, the separability was generally good except for *MIR*, *NDVI*, and *V2*. For the generally good indices, the trends after cut did not correlate with the age after disturbance or, if they did correlate, the ages of recovery were very high.

The summer indices had worse separability in general than the winter ones. The vegetation indices (*NDVI* and *V2*) had the worst separability, especially immediately after cut. *NIR*, *NDVI*, *V2*, and *Greenness* had very low or negative values for age of recovery, which indicated that the index values deviated from the intact forest with the time after cut. *Wetness* and *S3* had relatively good separability immediately after cut as well as high coefficients of determination in the trend after cut and medium ages of recovery (a few decades), which indicated they had clear

tendency of recovery within a couple of decades.

3.5 Discussion

3.5.1 Characteristics of the Indices

On a single winter image of TM96, all the indices except *MIR*, *NDVI* and *V2* separated the cuts and fires from the intact forest quite well, even nearly 15 years after disturbance. *RED*, *N-RED* and *Wetness* presented particularly good separability (Table 3.3). *NIR*, *Brightness*, and *Greenness* also presented reasonably good separability. They kept the separability throughout the images (Table 3.2), though the index values varied among the images (Figure 3.6), which might be caused by the conditions of atmosphere or snow, sensor degradation, sun incident angle *etc.* Only *N-RED* maintained good separability as well as stable index values throughout the images. *MIR* could not separate forest disturbance well because of the low reflectance of both forest and snow at the mid-infrared wavelength.

The good separability of these indices follows naturally from the fact that the reflectance of snow is much higher than that of forest at the visible and near-infrared wavelengths. However, caution must be exercised when using *NIR* or *Greenness*, because the reflectance of snow at the near-infrared can approach zero as the snow grain size becomes large (DOZIER, 1989); that is, high reflectance of snow at the near-infrared cannot be expected in late spring. Another consideration regarding the near-infrared bands should be that the reflectance of forest during winter might vary depending on whether the forest is evergreen or deciduous.

Though *NDSI* and *S3* showed good separability on TM96 (Table 3.3), the indices derived by division of the bands, that is, *NDVI*, *V2*, *NDSI*, and *S3*, generally had unstable values (high relative ranges of means) and poor separability over time (Table 3.2 and Figure 3.6). Particularly unstable were the intact forests, which had very low reflectance at any wavelength (see *RED*, *NIR*, and *MIR* in Figures 3.6 and 3.7). As denominators, the low reflectance pixels amplify their own random errors and/or the systematic errors introduced by the atmospheric correction more severely than the high reflectance pixels do when calculating the indices by division of the bands.

Therefore, the index values for the intact forest, which has low reflectance, and the separability of such forest from other forest classes both became unstable. Thus, it would be wise to avoid using those indices of winter images for forest monitoring.

The recovery after disturbance tended to be very slow or non-linear within the duration of the study, for each winter index. Even *NDVI*, *V2*, *NDSI*, or *S3*, whose coefficients of determination were relatively high (Table 3.3), did not show clear differences among the cut classes of different ages. This stability allows the disturbances to be detected for at least about two decades. However, it is not practical to use winter images to assess the early stage of succession of stands after disturbance because of the stability of the indices.

The summer indices behaved quite differently from the winter indices. In summer, *NDVI* of *0 – 6 years after cut* had as low a value as that of *Before cut*. The vegetation indices (*NIR*, *NDVI*, *V2*, and *Greenness*) showed a similar tendency in summer. Usually these indices dropped immediately after disturbance due to canopy removal, a characteristic that has been widely used to detect clear-cuts (COPPIN and BAUER, 1996; HAYES and SADAR, 2001; SADER and WINNE, 1992). However, these indices recovered rapidly and exceeded the original vegetation's value. The ages of recovery for those indices took low values, which suggests that the index values experienced drastic temporal change. WILSON and SADAR (2002) noted that changes in *NDVI* could be used to detect clear-cuts within only 1 – 3 years after cutting. In this study, the intervals of winter image acquisition were even longer, which made the vegetation indices fluctuate over the course of about 15 – 20 years. The chance of summer image acquisition was even worse than that of winter's. Thus, those vegetation indices in summer are not practical for detecting changes in forests of the region.

Summer *Wetness* showed a clear linear increase following a sharp drop to the bottom immediately after disturbance. The age of recovery for *Wetness* was 15.8 years, which means that by *11 – 16 years after cut* the index almost recovered to the value before cut. However, the index for *11 – 16 years after fire* remained low. Though the recovery of an index does not necessarily represent the recovery of the vegetation, as

pointed out previously, summer *Wetness* can be a good indicator of early succession after cut in the first decades. *MIR* correlates closely with *Wetness*, and many studies have pointed out the importance of *MIR* or *Wetness* in describing early forest succession (HAYES and SADAR, 2001; COHEN *et al.*, 1995; COLLINS and WOODCOCK, 1996; FIORELLA and RIPPLE, 1993).

From the discussions above, it can be summarized that boreal forest change can be best detected by using a time series of winter *RED*, *N-RED* or *Wetness*, and the early succession stage can be estimated by summer *Wetness* for the first few decades after cut.

3.5.2 Fire Scars on Winter Image

Fire scars could not be distinguished from cut stands by index values on winter images in which snow obscured the evidence of fire such as charring. In addition, because forest on the winter images is distinguished as tall and dark objects on snow regardless of whether they are dead or alive, the standing dead trees after fire are classified as forest. This might be why the clearing by a large fire was detected over the course of many years, despite the occurrence of the fire only once. To classify fire scars automatically and correctly, supplementary analyses of summer images are required. For example, old fire scars can be distinguished from a time series of summer images by *Wetness'* shallower trend of recovery than the trend for cuts. In summer images obtained immediately after fire, the fire scars can be detected by charring (ROY *et al.*, 2002).

3.5.3 Change Detection Using the Good Indices

The change detection of forest canopy in the study area from 1980 to 1999 was examined by using winter *N-RED* and *Wetness*, two of the indices recommended in the previous section. The changes of each period were derived from pairs of successive images. COHEN *et al.* (1998) recommended a simultaneous processing of multi-date images over merging the pair comparisons, however, the latter has its advantages in its simplicity and expandability to the future. Since fire scars could hardly be

distinguished from cuts, as mentioned previously, the fire scars were classified into one of the cut classes.

Since the *N-RED* had already been normalized, the changes were delineated by differencing the successive two indices followed by thresholding with an arbitrary fixed (threshold) value of 0.3. *Wetness* had good separability but was not stable throughout the images. Therefore, principal component analysis (PCA) was applied for each pair of successive *Wetness*, and the minor component was thresholded with two standard deviations to identify the changes. PCA shows the overall changes among images in the major component and the local changes in the minor component (SINGH, 1989).

The producer's accuracy was assessed by comparing the classification with the interpretation using the 60 preserved interpretation samples for each class (see Subsection 3.3.4). The user's accuracy was assessed by interpreting the random sample points on the classification result; with 100 points for each changed class and 400 points for each unchanged class (Table 3.4).

Both the indices showed almost same level of user accuracy (66 – 100%) and the producer's accuracies (79 – 98%). The later periods (*1990 – 1996*, *1996 – 1999*) had lower accuracies in general, and this is supposedly because the area of real cuts/fires had been reduced recently. The user's accuracy was better than producer's for all periods except 1996 – 1999, which suggested that the area of cut/fire was underestimated for those periods.

For change detection using *RED*, another good index, PCA should be applied, since *RED* was not stable, too (Figure 3.6, Table 3.2). The result was expected to be almost as same as that for *N-RED*, because each image's *RED* has a linear relationship with the corresponding *N-RED*. Note that PCA would not be simply applied for *RED* for MSS80, whose original band 5 saturated at high reflectance.

Given that the three indices had the almost same level of accuracy, *RED* and *Wetness* might have a better performance, because PCA and the derivation of *RED* and *Wetness* required neither manually nor subjective judgment, while *N-RED* required a time-consuming interpretation of snow distribution. On the other hand, *RED* and

N-RED required only a visible band. Especially *N-RED* could be derived from even the saturated band 5 of MSS80. With this flexibility of the relative normalization of a visible band, history of boreal forest would be able to be traced back to Landsat MSS of three decades ago, or even back to aerial and space photography of up to nearly a century ago.

3.6 Summary of Chapter

Using a time series of winter satellite images and a summer image for comparison, the author examined several indices (*RED*, *NIR*, *MIR*, *N-RED*, *NDVI*, *NDSI* (KLEIN *et al.*, 1998), SAITO and YAMAZAKI's (1999) *V2*, *S3*, and Tasseled Cap (KAUTH and THOMAS, 1976; CRIST *et al.*, 1985) *Brightness*, *Greenness*, and *Wetness*) for change detection in boreal forest in the Russian Far East.

The results show that;

- Winter *RED*, *N-RED*, and *Wetness* are the best indices for detecting canopy removal. The indices remain sensitive to the changes for at least about two decades. Both user's and producer's accuracies of the change detection with the indices were within 66 – 100%.
- *NDVI*, *NDSI*, and other indices derived by division are too unstable to distinguish changes from no changes.
- Using only winter image it is difficult to distinguish fire scars from cut stands or to estimate the succession stage after disturbance. It might be achieved in combination with summer image analysis.
- Summer *Wetness* is the best index for identifying recovery after disturbance within a few decades.

These results can be applied to the management of boreal forest covered by snow every winter. Use of winter images enabled change detection even after the passage of many years. Thus, it can be used to reconstruct the forest management/disturbance history by using images taken during the more than three decades of Landsat operation, or even longer with aerial and space photography.

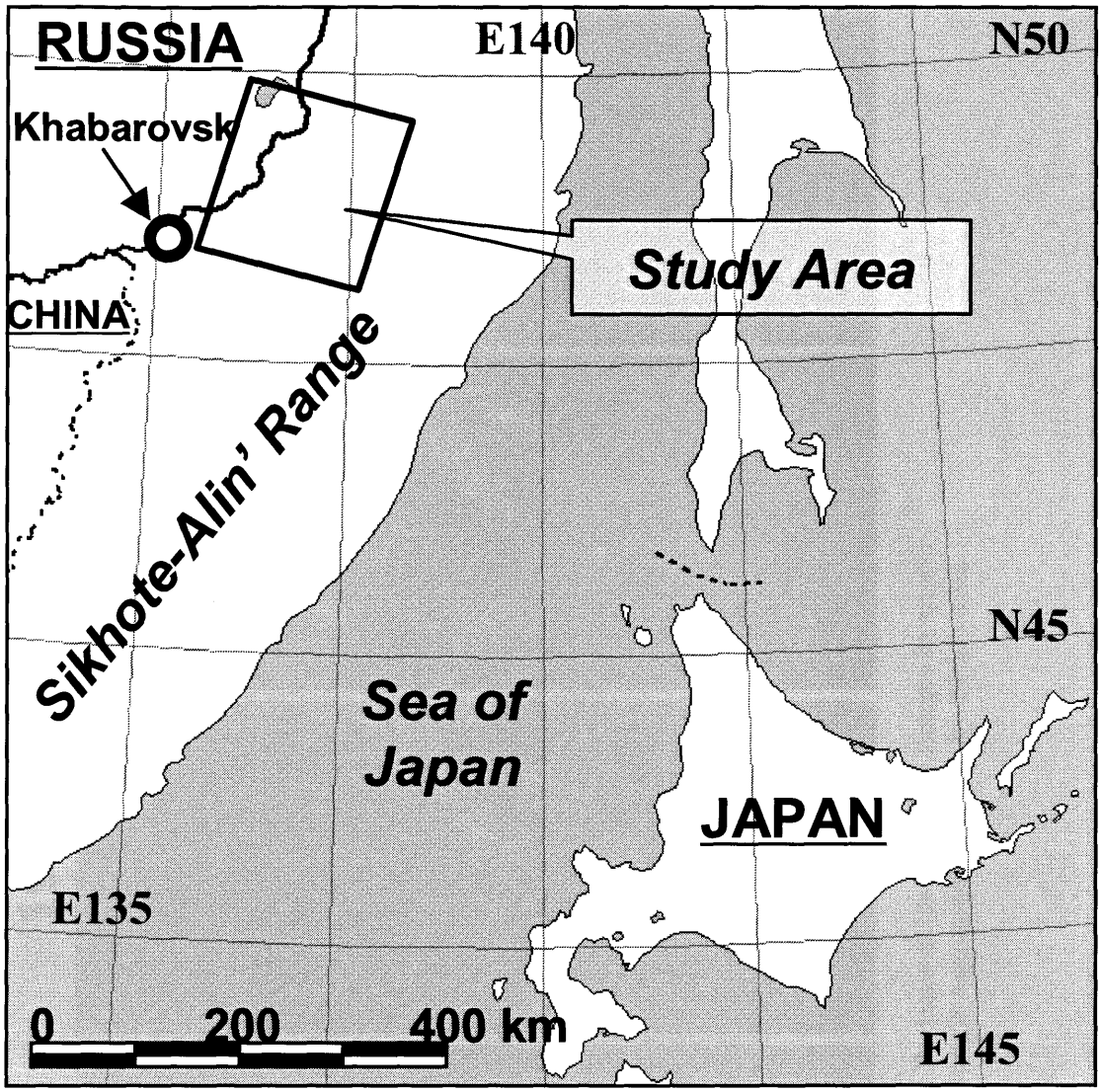

Figure 3.1 Study area

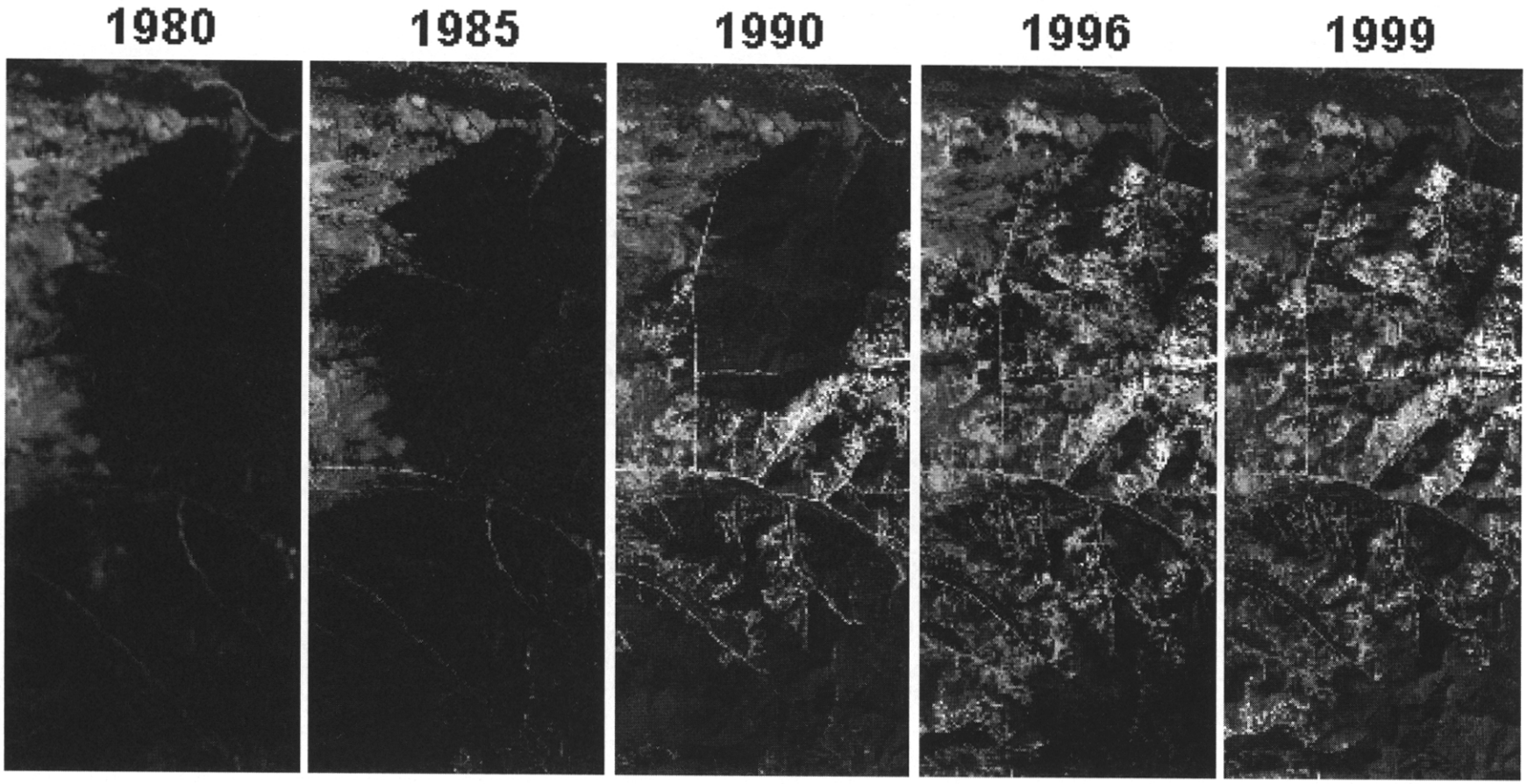

Figure 3.2 Portions of the red band images in winter
Each rectangle represents a 10-km by 24-km area.

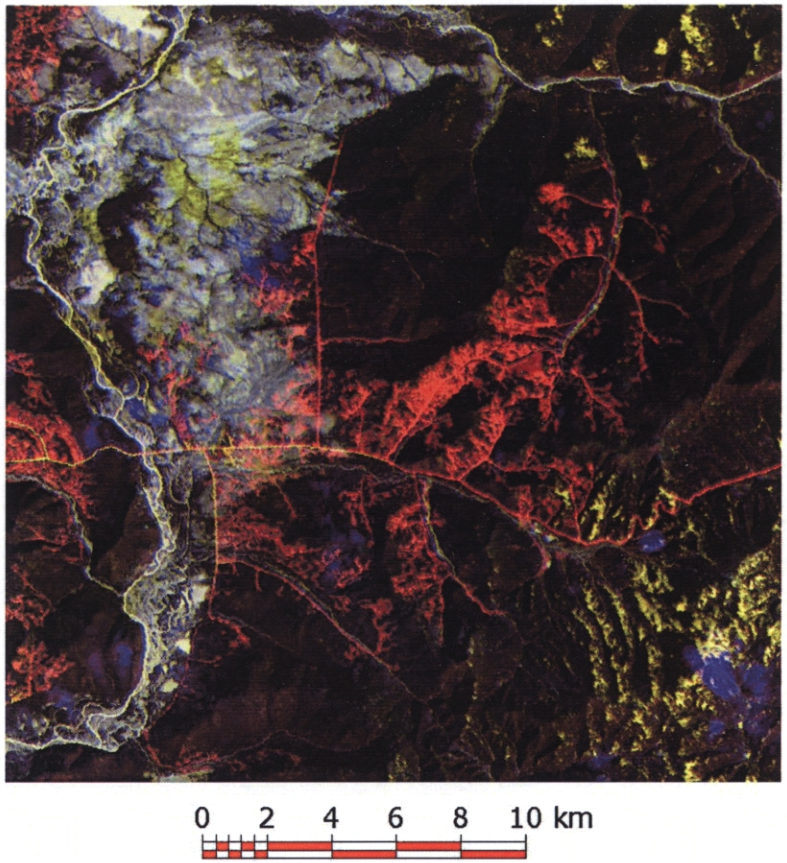

(a) Blue: 1980 – Green: 1985 – Red: 1990
Yellowish: cut during 1980-1985,
Reddish: cut during 1985-1990

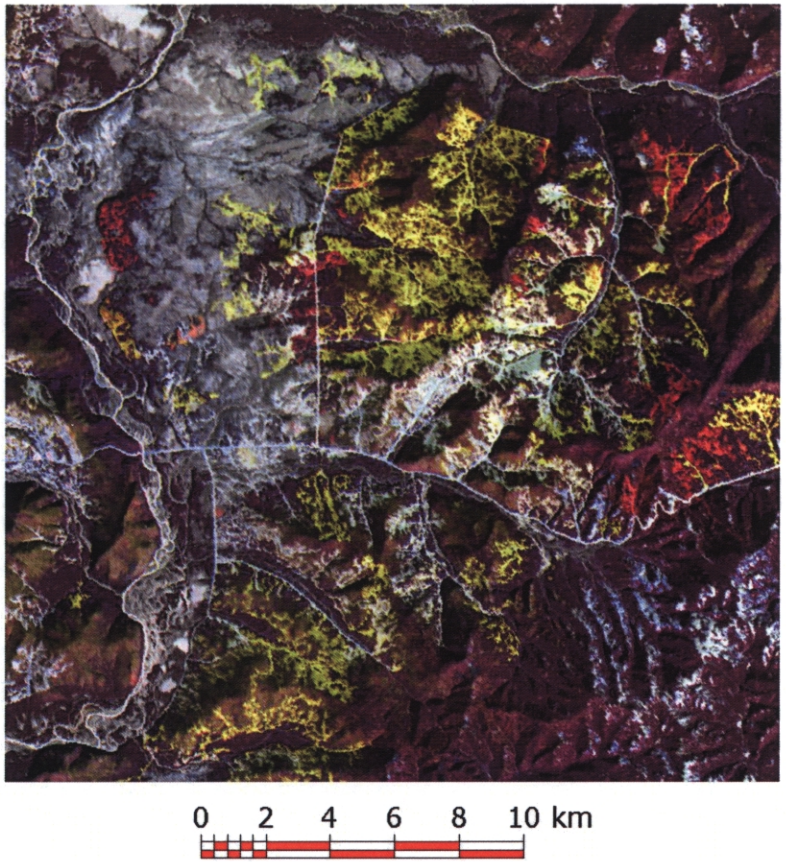

(b) Blue: 1990 – Green: 1996 – Red: 1999
Yellowish: cut during 1990-1996,
Reddish: cut during 1996-1999

Figure 3.3 Color composites of the red bands for the change interpretation
The area of Figure 3.2 is included as a part.

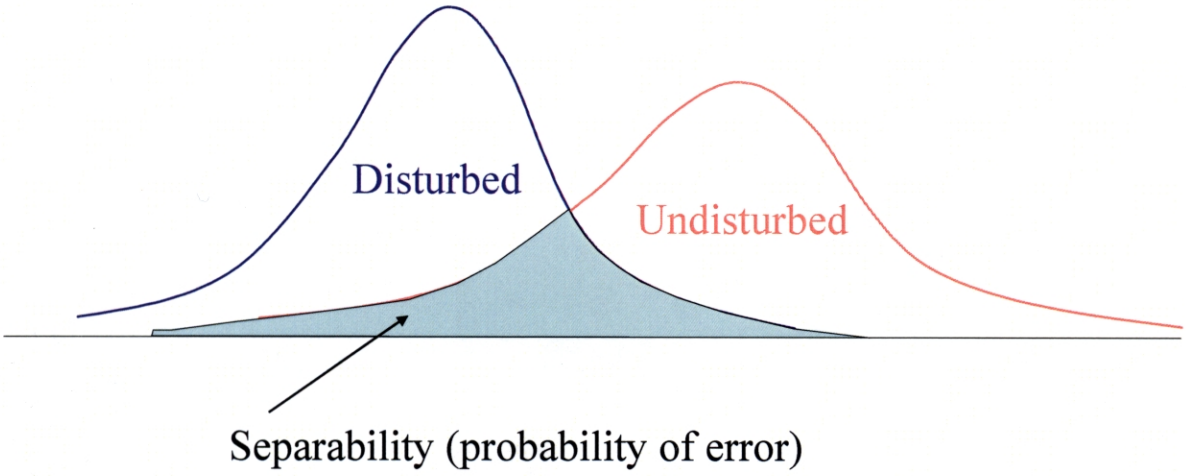

(a) A single-year comparison of the disturbed and undisturbed stands using an index

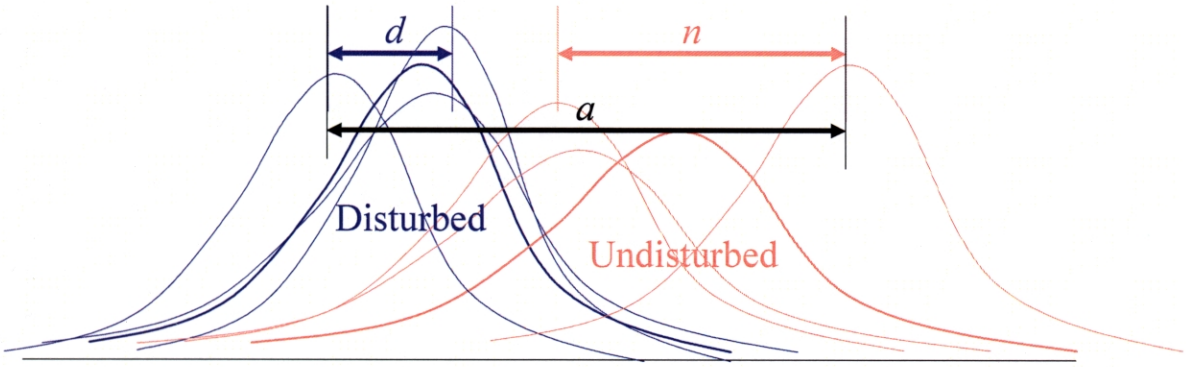

(b) A multi-year comparison of the disturbed and undisturbed stands using an index

The relative range of means, *RR*, is represented as *d*/*a* for the disturbed stands and *n*/*a* for the undisturbed stands..

Figure 3.4 Preferable properties of indices for detecting forest disturbances

In a single-year comparison, the probability of error for misclassification is represented as the overlapped area of the two distributions: the better index has the less probability of error. In a multi-year comparison, stability and reproducibility of an index for a class is preferable. Thus, the better index has the less relative range of means.

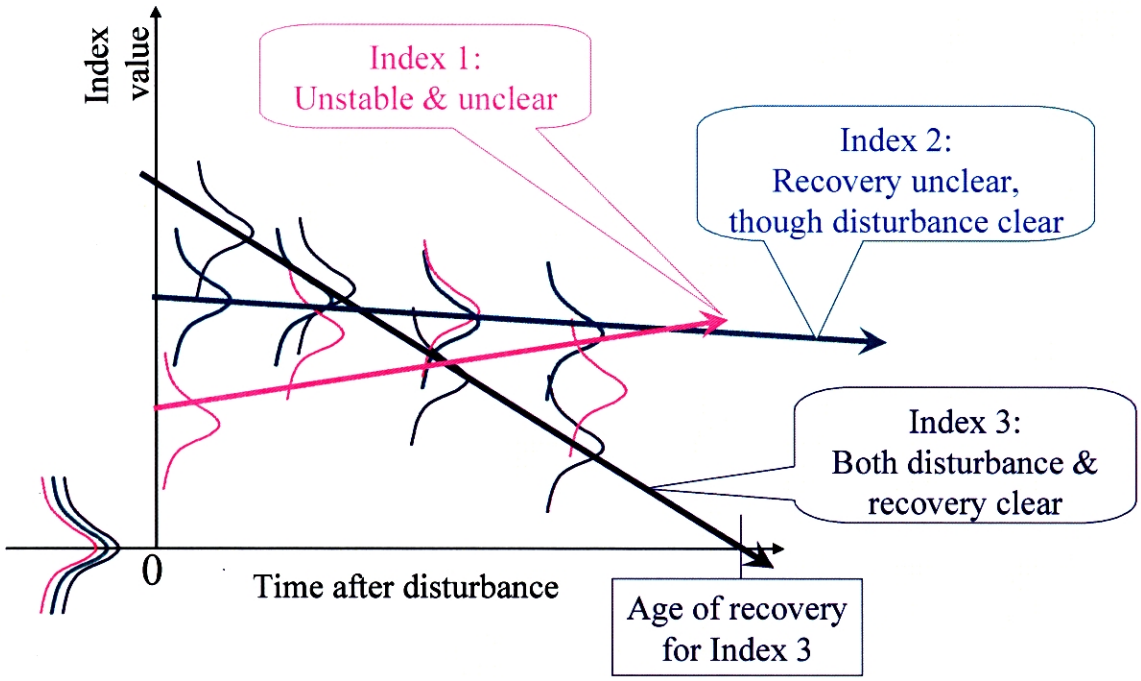

Figure 3.5 Preferable trends of indices for detecting the recovery of forest after a disturbance

Index 1 (purple) is not a suitable indicator of recovery because it does not show a monotone recovery to the pre-disturbance (intact) level. Index 2 shows a monotone but too gradual recovery for the duration of observation. Index 3 is a suitable indicator of recovery that shows a monotone and clear recovery to the pre-disturbance (intact) level within the duration of observation. The age of recovery is the age after disturbance on the regression line at which the index value recovers to the pre-disturbance (intact) level.

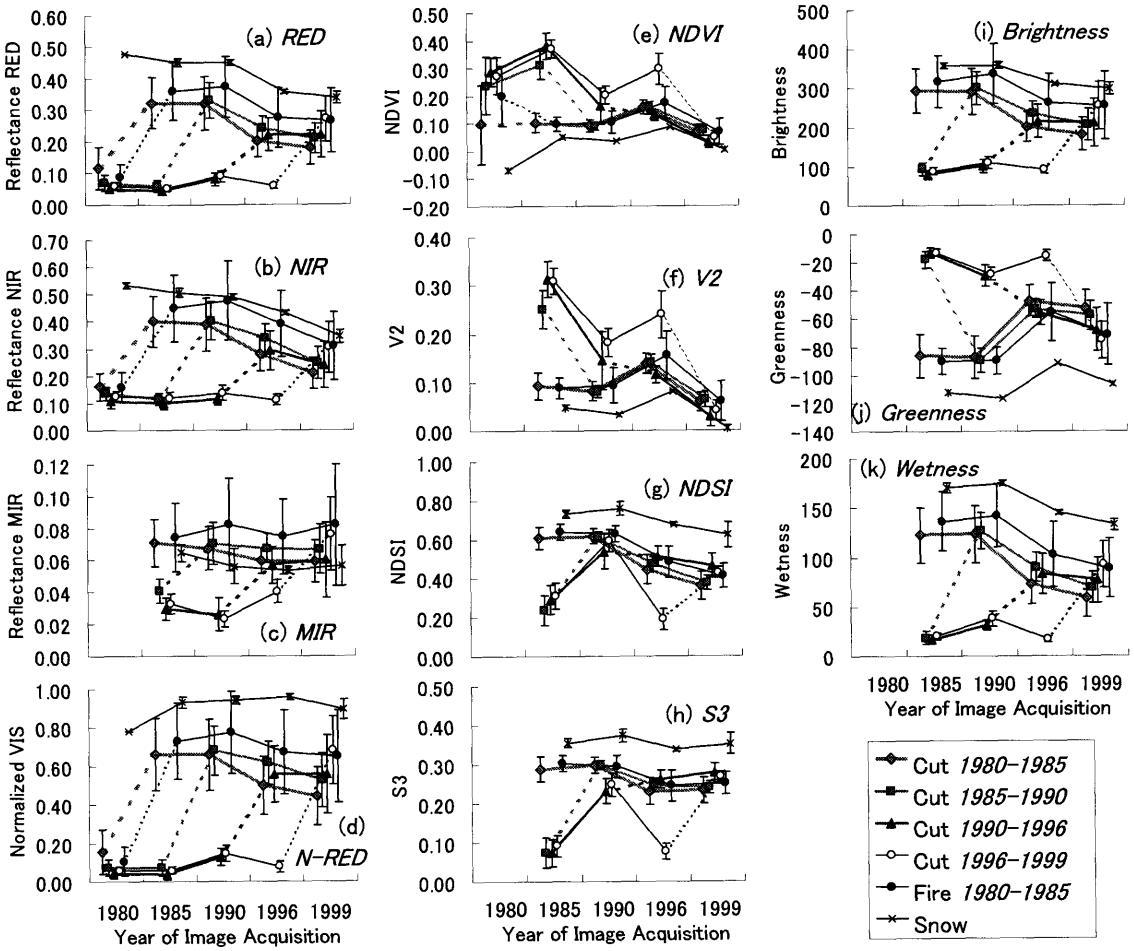

Figure 3.6 Time series of indices of the forest stands with different disturbance occurrence time/disturbance type. Vertical bars indicate standard deviation. Dashed lines indicate that cut/fire occurred during the period covered by the lines. n = 60 for each class.

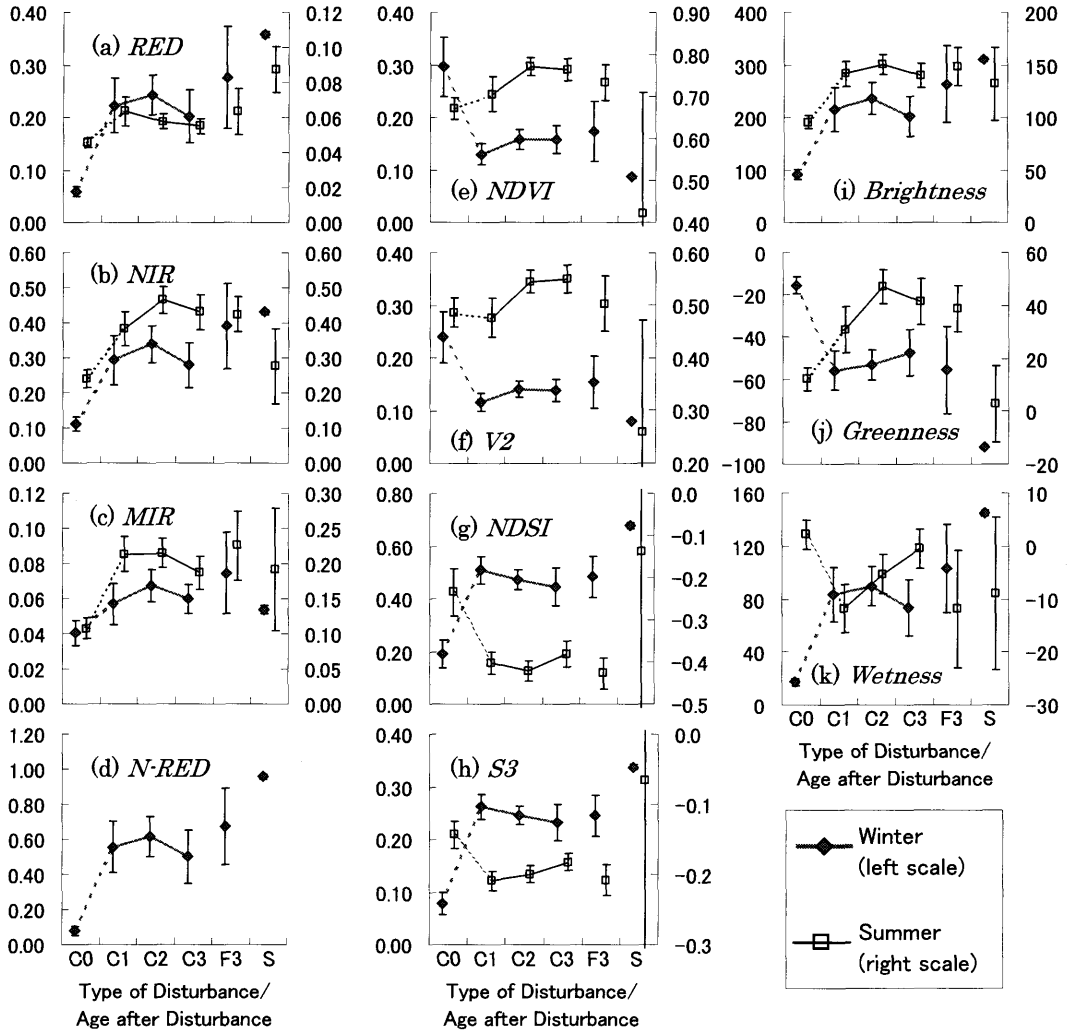

Figure 3.7 Chronosequence of indices of the forest stands with different type of disturbance/ age after disturbance, derived from TM96 (winter) and TM95S (summer). The vertical scales at left and right are for winter and summer indices, respectively. Vertical bars indicate standard deviation. Solid lines connect cut stands of different age. Dashed lines indicate that cut occurred during the period covered by the lines. n = 60 for each class. C0: Before cut (Cut *1996 – 1999*), C1: *0 – 6* years after cut (Cut *1990 – 1996*), C2: *6 – 11* years after cut (Cut *1985 – 1990*), C3: *11 – 16* years after cut (Cut *1980 – 1985*), F3: *11 – 16* years after fire (Fire *1980 – 1985*), S: Snow. *N-RED* was not derived for the summer image when snow was absent.

Table 3.1 List of satellite images used

Sat.	Sensor	Date	Path	Row	ID
L-3	MSS	80/03/19	121*	026*	MSS80
L-5	TM	85/03/15	112**	026**	TM85
L-5	TM	90/03/13	112**	026**	TM90
L-5	TM	96/03/13	112**	026**	TM96
L-5	TM	99/02/18	112**	026**	TM99
L-5	TM	95/07/17	112**	026**	TM95S

Note: L-3: LANDSAT3, L-5: LANDSAT5, * WRS-1, ** WRS-2

Table 3.2 Separability and stability of indices over time

	probability of error in separating cuts and fires from forest [%]			Relative range of index means of the classes across the images [%]		
Index	TM85	TM90	TM96	Forest	Cut/Fire	Snow
RED	0.4	0.9	0.7	16.8	45.3	31.7
NIR	0.9	1.8	1.8	14.1	62.0	43.3
MIR	10.4	6.6	18.2	30.0	42.8	18.3
N-RED	0.4	0.9	0.7	12.8	36.0	19.3
NDVI	0.6	27.2	13.9	63.0	31.3	35.1
V2	1.0	27.9	19.3	54.3	40.8	25.1
NDSI	0.8	36.8	2.2	70.8	49.2	24.1
S3	0.1	20.1	0.3	58.0	23.2	11.9
Bright.	0.2	0.6	1.2	11.0	55.5	21.3
Green.	0.1	0.4	3.7	15.9	41.6	23.8
Wet.	0.1	0.9	0.6	13.9	52.7	26.6

Table 3.3 Separability and succession trend of the chronosequences of disturbance

		Probability of error 'Before Cut' versus			Trend after Cut		
	Index	0-6 yrs after Cut	11-16 yrs aft. Fire	Snow	*R*		Age of recovery [yr]
Winter	*RED*	0.3%	1.1%	0.0%	0.02	*	94.1
	NIR	1.8%	1.6%	0.0%	0.00		
	MIR	18.2%	10.6%	6.8%	0.01		
	N-RED	0.3%	1.1%	0.0%	0.02	*	94.1
	NDVI	1.3%	13.9%	0.0%	0.21	**	62.0
	V2	2.6%	19.3%	0.0%	0.20	**	56.4
	NDSI	0.1%	1.3%	0.0%	0.18	**	54.9
	S3	0.0%	0.3%	0.0%	0.18	**	67.2
	Bright.	0.6%	1.2%	0.0%	0.01		
	Green.	0.1%	3.7%	0.0%	0.12	**	54.2
	Wet.	0.1%	0.5%	0.0%	0.03	**	81.0
Summer	*RED*	5.2%	9.4%		0.25	**	24.5
	NIR	2.6%	0.7%		0.12	**	-31.6
	MIR	0.4%	2.9%		0.16	**	47.2
	NDVI	28.8%	17.7%		0.33	**	-5.1
	V2	41.0%	33.1%		0.47	**	3.0
	NDSI	2.0%	2.0%		0.06	**	98.4
	S3	2.0%	5.7%		0.43	**	29.4
	Bright.	0.5%	1.3%		0.00		
	Green.	7.0%	1.9%		0.18	**	-17.9
	Wet.	2.6%	10.8%		0.57	**	15.8

Note: the winter and summer images are TM96 and TM95S, respectively

Table 3.4 Accuracies of the change detections using "good" indices

	N-RED		*Wetness*	
Period	User's	Produc-er's	User's	Produc-er's
1980-1985	94.1%	81.5%	N/A	N/A
1985-1990	99.0%	97.2%	87.9%	97.6%
1990-1996	100.0%	79.8%	89.0%	85.6%
1996-1999	65.7%	97.2%	74.7%	78.5%
No Change	90.7%	N/A	99.0%	N/A

Note N/A = "not available"